Research Article | Vol. 11, No. 12 / 1 December 2020 / Biomedical Optics Express 7019
Biomedical Optics EXPRESS

Optical detection of formaldehyde in air in the 3.6 µm range

MATEUSZ WINKOWSKI* AND TADEUSZ STACEWICZ

Institute of Experimental Physics, Faculty of Physics, University of Warsaw, Pasteura 5, 02-093 Warsaw, Poland
*mateusz.winkowski@fuw.edu.pl

Abstract: The optical detector of formaldehyde designed for sensing cancer biomarkers in air exhaled from human lungs with possible application in free atmosphere is described. The measurements were performed at wavelengths ranging from 3595.77–3596.20 nm. It was stated that at the pressure of 0.01 atm this absorption band exhibits the best immunity to typical interferents that might occur at high concentration in human breath. Multipass absorption spectroscopy was also applied. The method of optical fringes quenching by wavelength modulation and signal averaging over the interferences period was presented. The application of such approaches enabled the detection limit of about single ppb to be achieved.

1. Introduction

Sensitive and fast detection of trace gases is useful for many applications, including industrial and agriculture processes control, environmental monitoring, detecting of toxic compounds and medical implementation [1–3]. Among various constituents the identification of formaldehyde (H_2CO) belongs to the most desirable. This gas is toxic, mutagen and possibly carcinogen. It is frequently used in chemical industry. For instance it is used for household materials (furniture and paints). Its emissions during production and from the products can affect human health and cause discomfort, irritation of eyes, nose, and throat, leading to sneezing and coughing [4–9]. It also contributes to the "sick building syndrome" [10,11]. The number of patients allergic to formaldehyde is still increasing in many industrial countries with air pollution problems [12–15].

Formaldehyde concentration levels in urban environment ranges typically from about 2 to 45 ppb, which is primarily due to industry and emissions from vehicles. The secondarily source is the photochemical oxidation of volatile organic compounds at intense sunlight [16]. Typical H_2CO concentrations are 10–80 ppb in normal indoor conditions, however it can reach 80–300 ppb in polluted case. The World Health Organization (WHO) has set a 30 min exposure limit of 80 ppb [17]. According to American Conference of Governmental Industrial Hygienists (ACGIH) formaldehyde concentration should not exceed 300 ppb at any time. Monitoring of H_2CO in the troposphere with ppb and sub-ppb resolution is also important for understanding of its role in ozone formation mechanism [18]. Therefore, potential sensitive formaldehyde detection with a fast time response is desired and versatile. This detection includes industrial and environmental monitoring as well as indoor and urban air quality observations.

Formaldehyde has also been identified as a potential lung and breast cancer biomarker in breath analysis [19–24]. Therefore a sensitive and reliable human breath H_2CO sensor can provide a promising method for non-invasive, real-time and point-of-care disease diagnostics and metabolic status monitoring it can also be used as a screening test for primary or metastatic cancer [25]. Morbid level of formaldehyde concentration is not well established. Early findings claimed that in exhaled breath from breast cancer patients, H2CO concentration of 0.45–1.2 ppm was observed compared to normal levels of 0.3–0.6 ppm [26,27].

Several different chemical and physical methods have been used. Liquid chromatography [28,29], gas chromatography [30–32] and ion chromatography [33] can provide ppb and sub-ppb

#405384 https://doi.org/10.1364/BOE.405384
Journal © 2020 Received 13 Aug 2020; revised 29 Sep 2020; accepted 9 Oct 2020; published 10 Nov 2020

Biomedical Optics EXPRESS

detection sensitivity. However the large weight and size of such equipment and long measurement times are negative aspects associated with these methods. These methods are also expensive and require qualified staff. Semiconductor gas sensors based on gas-sensitive films are a good alternative for formaldehyde monitoring due to their short response time [34–36], however their selectivity and relatively high detection limits (>250 ppb) are the limitations. Electrochemical H2CO sensors are of good sensitivity and selectivity, but are limited by poor temporal stability (with a time response of one hour) [37,38]. Chemical analyzers, which employ coloration of a formaldehyde sensitive reagents, are also sensitive at ppb levels but their results might be interfered by other organic compounds and require long sampling times (i.e. minutes or more). Very sensitive sensors of H_2CO (0.1 ppb) based on fluorescence induced by 353–355 nm laser pulses were also constructed for atmospheric purposes [39–41].

Optical approaches to trace matter detection might lead to high selectivity, good selectivity and fast response time (of less than one minute.). Here the application of mid-infrared spectroscopy is especially interesting. Strong and narrow optical absorption lines corresponding to rotational-vibrational transitions between the levels of the molecules of interest are located there. These transitions provide molecular fingerprints of the constituents. Single pass spectrophotometry and polarography [42] are powerful analytical techniques that allows the quantitative speciation of gas mixtures, but are characterized by insufficient sensitivity. However the application of various ultrasensitive methods of laser spectroscopy enable good results. Recent progress in optoelectronics provides an opportunity to construct relatively simple biomarker sensors which allow to detect sub-ppb concentrations [43].

Cavity ring-down spectroscopy is the most sensitive (but the most complicated) method of laser absorption spectroscopy. The gas sample is located in optical resonator consisting of mirrors of very high reflectivity. Laser light is used to determine the resonator quality factor. Such parameter decreases when the losses coefficient (i.e. the absorption) increase. A comparison of the Q-factor for empty cavity with one registered in the presence of investigated gas provides opportunity to determine absorption coefficient of the sample. The sensitivity of CRDS systems is practically about 4∼5 orders of magnitude better than one of single pass spectrometry [44–48].

Photoacoustic spectroscopy (PAS) is another sensitive approach that has also been applied for formaldehyde detection [49,50]. Amplitude modulated light beam is introduced to the cell in this method. Absorption of the radiation induces synchronous acoustic wave which is registered with a sensitive microphone. Registration sensitivity might be increased many times when the sample is located in acoustic resonator and the modulation frequency is matched to this resonance. Additionally the replacement of the microphone by a resonant quartz tuning fork leads to further sensitivity improvement (QEPAS) [51].

Multipass spectroscopy is also a sensitive methods [52,53]. High sensitivity is achieved due to light path lengthening in the experimental cell containing the investigated gas sample. The cell is ended with two concave mirrors with broadband coatings. A laser beam is introduced through a small hole in one mirror and its reflection is then multiplied among the mirrors. As a result the light path might be lengthened tens or ever hundreds of times inside the sample in comparison with common single-pass cell. The absorption coefficient is found from the Lambert – Beer absorption law.

In this paper we present our approach - high sensitivity sensor of formaldehyde based on multipass spectroscopy. Technique of optical interferences quenching was applied. The construction was designed for cancer biomarker detection in air exhaled from human lungs with possible application in free atmosphere.

2. Spectrum analysis

High sensitivity optical detection requires a choice of a strong absorption band (fingerprint) of constituent of interest. One has to avoid the disturbance by other species which might be present

Biomedical Optics EXPRESS

in the investigated sample. This is especially important in the case of breath analysis with more than 3000 various constituents already detected in exhaled air [54].

The absorption spectrum of formaldehyde in mid-IR consists of two bands situated close to 3500 nm and 5800 nm [55]. The long wavelength band however is strongly affected by H2O absorption. Water vapour concentration in free atmosphere is usually above 0.1%. While in breath it can reach up to 5%, so it exceeds the formaldehyde density by many orders of magnitude. Moreover, in such long wavelength range the use of special optical materials is necessary, complicating the experimental scheme.

Shorter wavelength band of H_2CO is weaker but often used for optical detection of this compound [56–63]. It is minimally affected close to 3595.8 nm (Fig. 1(a)), however it is still interfered by strong absorption of H2O, CO2 (both up to ~5% in breath) and CH4. Therefore the optical detection of H_2CO with the sensitivity of tens of ppb is impossible in normal pressure conditions.

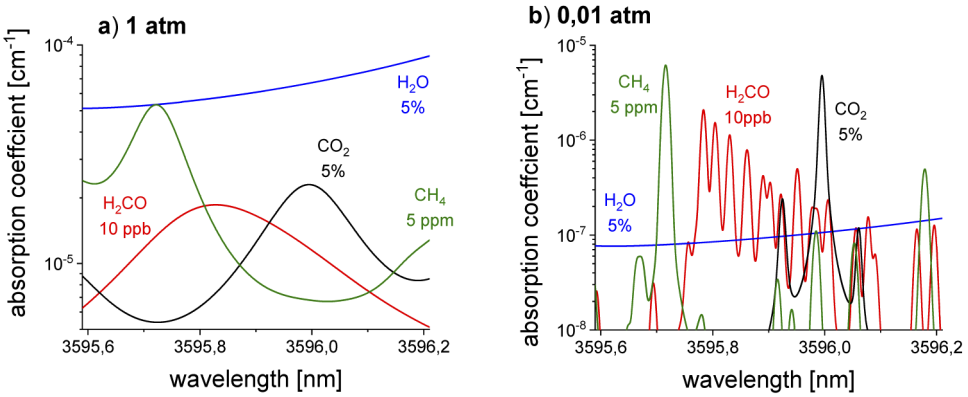

Fig. 1. Absorption spectrum of formaldehyde and typical interferents present in breath: a) at normal atmospheric pressure; b) at the pressure reduced to 0.01 atm [55].

Molecular collisions are mainly responsible for spectral line shapes in the air samples [64]. The air pressure diminishing in the sample can efficiently reduce the collisional line broadening. In Fig. 1(b), the relevant spectra of H_2CO in air at the pressure of 0.01 atm are shown. Pressure broadening was reduced many times which narrowed the absorption lines of the constituents and caused their separation. Relative value of H_2O, CO_2 and CH_4 backgrounds were diminished about one hundred times. Due to that sensitive optical detection of formaldehyde might be performed within the wavelength range of 3595.77–3596.20 nm. Although this is not the strongest line group in the formaldehyde spectrum, we found that it is the least of all interfered in 3500 nm band. Therefore, it this the best for detection of trace amounts of this biomarker in the air exhaled from the lungs.

3. Experimental

3.1. Experimental setup

A simplified scheme of the experimental setup is presented in Fig. 2. A 3 mW, CW tunable laser (Nanoplus ICL IR) generating radiation within the range of 3596 - 3598 nm was applied. Coarse tuning of the laser with a temperature controller (Toptica DCT 110) was used to stabilize its wavelength near the center of the absorption band. Fine control of the wavelength (with precision of 0.001 nm) was performed by a current controller (Thorlabs TLD001). The laser current was modulated with a two channel function generator (Tektronix, AFG3102). One channel (frequency 91 Hz) served for the laser diode scan across the formaldehyde spectrum. The second channel

Biomedical Optics EXPRESS

(10 kHz) was used for optical interferences quenching (described in Section 3.2). Output signals from both channels were combined with a different weights in custom summing amplifier.

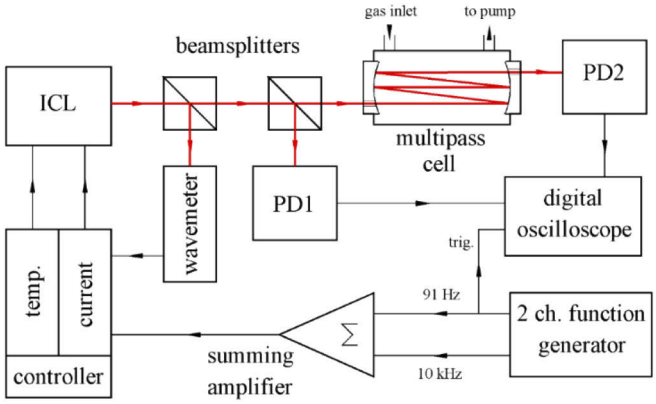

Fig. 2. Simplified scheme of the experimental system.

The laser beam passed through two beamsplitters. The first one directed a part of the beam to a wavemeter (HighPrecision, model WS-6IR) that was used for laser wavelength measurement. The other beam splitter together with photodetector PD1 (Thorlabs, PDA20H) was applied for monitoring of laser power before introduction to a multipass cell. A custom developed vacuum Herriot cell was constructed with two spherical mirrors which had a curvature radius of 2 m. The distance between the mirrors was 65 cm. The optical path length reached 17.5 m. The intensity of the light beam leaving the cell was detected with photodetector PD2. A digital oscilloscope (Tektronix DPO7000) was used for signal acquisition.

An Investigation of ICL laser was performed. We stated a nonlinearity of both power and wavelength versus the supply current (Fig. 3). Therefore, higher harmonics occur in photodetector signals when modulating the laser with a sine wave. This complicates using wavelength modulation spectroscopy (WMS), especially its 2f variant.

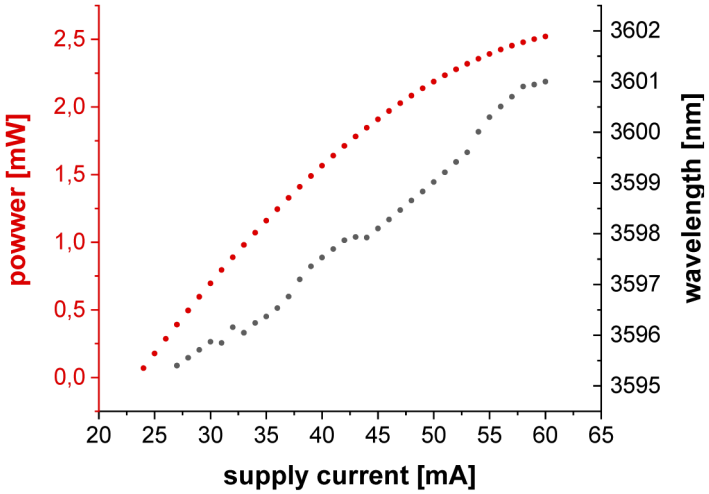

Fig. 3. ICL power and wavelength versus the supply current.

Biomedical Optics EXPRESS

WMS-2f consists in laser wavelength modulation within the absorption line. This leads to intensity modulation of the beam passing through the absorption cell. Phase sensitive detection (lock-in) is applied for signal acquisition. In the case of using the laser that changes the wavelength and power linearly with the supply current, the amplitude of second harmonics is proportional to absorber concentration. Moreover, changes of the laser power with the supply current are compensated. This method is widely applied for trace mater detection due to its immunity to noises [75–80]. In our case, the nonlinearity of laser characteristics provide an additional signal at 2f frequency that strongly limits the sensitivity of this approach.

The nonlinearity of the laser forced us to develop another measurement method. 91 Hz sine signal from the generator (Fig. 2) scanned the laser wavelength across absorption spectrum of formaldehyde, i.e. within 3595.77–3596.20 nm. The signal from photodiode PD2 was averaged by the digital oscilloscope. Further elaboration of such data required removing of the background caused by laser power modulation. For that purpose a polynomial was fitted to the signal, which was then subtracted from the collected data. Then the excess white noise was removed with a properly selected low-pass filter. Due to that, the characteristic spectrum of formaldehyde was found. The fragment between the first and fourth minimum (see Fig. 1(b)) was separated. The data prepared in this way was then numerically integrated. The result was compared with the results registered for the 1 ppm calibrated mixture in order to determine H_2CO concentration.

During this procedure the result was compared with the reference spectrum from the HITRAN database [55]. Note, that due to using of the optical interferences quenching, the shape of the reference spectrum was modified according to the description presented in the next chapter.

3.2. Optical interferences quenching

Optical interferences, also known as fringe interferences, are the effects which can seriously spoil the accuracy of the experiment. The fringes are widely known as being generated in glass plates due to the overlapping of the beams which are reflected multiple times among its surfaces. This leads to modulation of the plate transmittance, according to formula: $T(\lambda) = [1 + Fsin^2(\delta/2)]^{-1}$, where $F = 4R/(1-R)^2$ denotes the finesse of the fringes, while R is the reflection coefficient [65]. The parameter: $\delta = 4\pi nd/\lambda + \Delta\varphi$. The refraction coefficient is denoted here by n while λ is the wavelength. The fringe phase shift $\Delta\varphi$ follows from uncertainty and thermal expansion of the distance between the reflecting surfaces (d). Wavelength difference among the maxima of the two neighbour fringes is equal to $\Delta\lambda \approx \lambda^2/2d$ (Fig. 4).

Experiments with multipass cells are often affected by this phenomenon. Inside the cells the light beams are spread due to diffraction as well as due to scattering on mirror surface imperfections, on other elements of the cell construction or just in the medium filling the cell. Scattered light overlaps on different light spots on the mirrors, leading to unexpected interferences. While the multipass cells are used for trace gases detection, usually its transmission is weakly modulated by the absorption of the gas sample. Additional modulation by such interferences might strongly reduce the sensitivity of this approach (Fig. 4). The fringes phase $\Delta\varphi$ is temporarily unstable due to the thermal expansion of the cell length and acoustic vibrations.

Many research groups have tried to solve this problem in different ways [66,67]. The simplest method consisted in the limitation of spot numbers on the mirrors. However, this metod also shortens the optical path and thus reduces the sensitivity. Another possible solution is to limit the laser beam diameter, but this leads to diffraction and formation of the Airy discs that may interfere with other spots. There are also solutions based on the application of special masks inside the multipass cell which separate the beams corresponding to different spots [68,69]. The active approaches consist in the periodic shifting of one of the mirrors by piezoelectric elements [66,70] or by fast pressure driven elements [71]. Oscillating Brewster plates or lenses are also applied [72,73]. This spoils stability of the interference fringes, and reduces the modulation when

Biomedical Optics EXPRESS

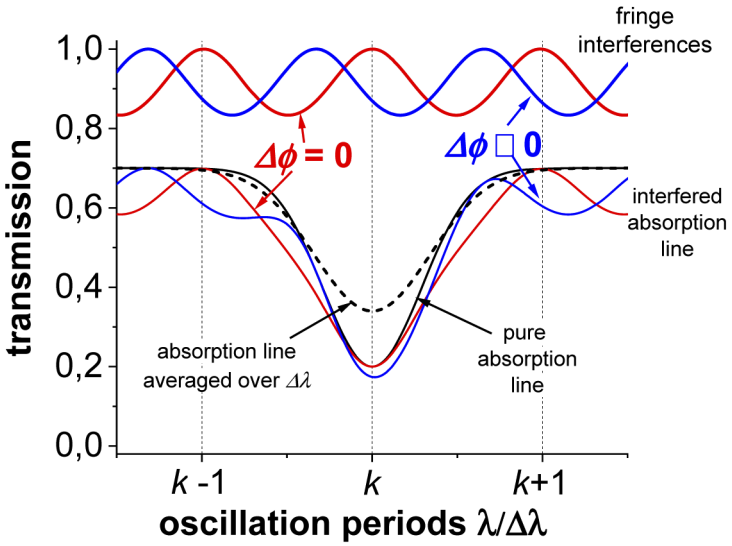

Fig. 4. Example of absorption line affected by optical interferences for two different phase shifts. The wavelength is determined by oscillation period number: $k = \lambda/\Delta\lambda$.

averaging the light transmitted though the cell. The downside of these methods is a significant system complication.

The reduction of optical interferences by laser wavelength modulation was also proposed [74]. We found that such modulation and signal averaging over the wavelength range ($D\lambda$) equal to the multiplicity of the fringes period is the most effective. From a mathematical point of view, the method is based on the theorem that the averaging of any periodic function over its period (or multiplicity of the period) provides the mean function value. The result is constant and independent on the starting point of the averaging.

Effects of this approach are presented in Fig. 5. Changes of transmission of an optical device affected by the interference considered above as a function of averaging range are shown for

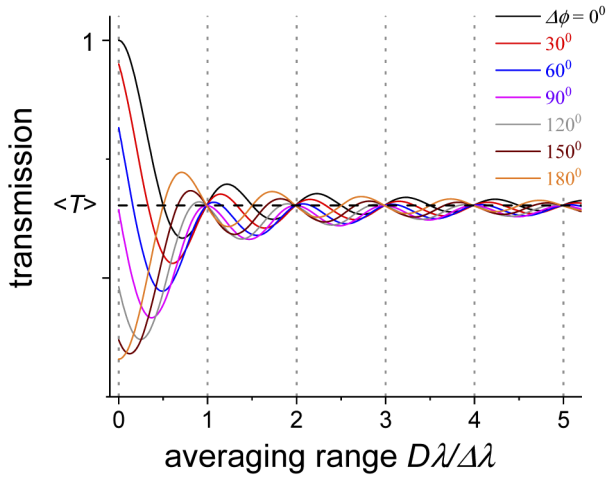

Fig. 5. Quenching of optical interferences due to wavelength modulation and signal averaging for various phase shifts.

Biomedical Optics EXPRESS

various $\Delta\varphi$ values. The most effective is the averaging over the wavelength range equal to multiplicity of the fringe period ($D\lambda/\Delta\lambda = 1, 2, 3\ldots$), since in this case the transmission does not depend on the phase shift and it is equal to a mean value $T = (1 - R)^2$.

A sine signal of 10 kHz was applied in our experiment for this purpose. Its amplitude, i.e. the range of modulation, was adjusted manually, through looking on the oscilloscope screen for the best minimization of interferences. It corresponded to $\Delta\lambda_{opt} = 0.011$ nm. There is about 10% discrepancy between measured value $\Delta\lambda_{opt} = 0.011$ nm and the $\Delta\lambda = \lambda 2/2d = 0.00994$ nm calculated for our multipass cell of d = 65 cm. It follows from the cell construction. The mirrors were 65 cm apart, but the surfaces of the metal mirror handles were approximately 8 cm closer to each other. That shows, the fringes were generated due to laser light scattering on these handles. This signal was combined in summing the amplifier with a 91 Hz signal serving for wavelength scanning across the formaldehyde spectrum. The amplifier output was connected with current control module and drove the laser. The averaging (over 1000 samples) was performed with a digital oscilloscope.

In Fig. 6, the spectra of laser light losses registered in a multipass cell filled with 1 ppm of formaldehyde in air at 0.01 atm is presented. The upper curve corresponds to the registration achieved without fringes suppression while the lower curve represents the spectrum purified by 10 kHz laser wavelength modulation.

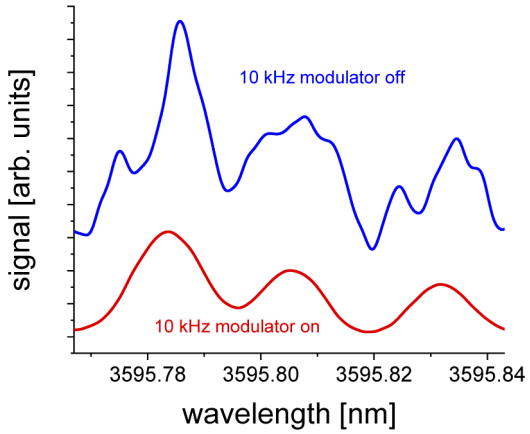

Fig. 6. Quenching of optical interferences in transmission spectrum of multipass cell filled with 1ppm of formaldehyde.

The application of averaging over a certain range of wavelengths leads to the spectral lines broadening and flattening. This was already shown in Fig. 7. Such broadening should be taken into account when comparing the registered spectrum with the reference spectrum. Therefore, preparing the reference spectrum HITRAN data was averaged over the range $\Delta\lambda_{opt} = 0.011$ nm. The shape of this curve (Fig. 6) coincides well with the reference spectrum of H_2CO from the HITRAN database [55]. A correlation coefficient of 99% was achieved.

3.3. Results and discussion

Correction over the spectrum amplitude must be performed when the concentration of the constituent is based on amplitudes comparing between the reference spectrum and the measured spectrum. In our case, a calibrated mixture of 1 ppm of H_2CO in nitrogen (Messer, precision 10%) was used as a reference. As it was stated before, we performed the investigation of our formaldehyde sensor at the pressure of 0.01 atm. In order to study the sensor output for different H_2CO concentrations a following procedure was conducted. In the first step the sensor was filled

Biomedical Optics EXPRESS

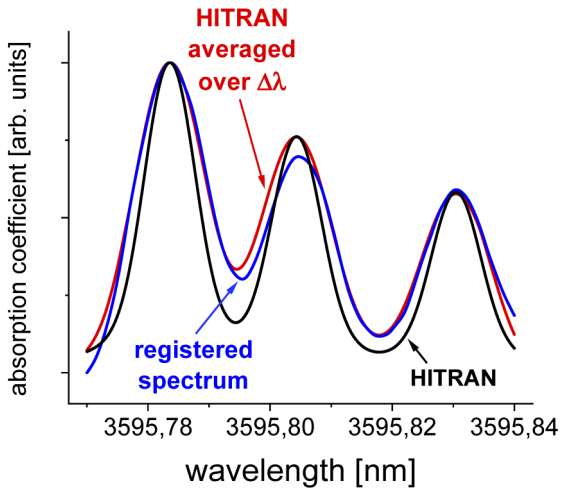

Fig. 7. Comparison of experimentally registered H_2CO spectrum with HITRAN reference spectrum and the reference spectrum averaged over $\Delta\lambda_{opt}$ range.

with this mixture. Therefore, the initial formaldehyde concentration was $2.7{\cdot}10^{11}$ cm^{-3}. After collecting the signal, the mixture was diluted with pure nitrogen evaporated from its liquid phase. The pressure was raised twice. After a time period of about 15 min, which was necessary to achieve a good mixing of the gases, the pressure was reduced again to the value of 0.01 atm. Precise dosing valves were used at the input and output of the cell. This ensured an appropriate flow rate of gas filling and pumping, and enabled the pressure control with a precision of 10^{-5} atm. The MKS Baratron (model 102A) was used to measure it. We expected that in this way a new mixture would be achieved with the half density of formaldehyde in respect to the previous

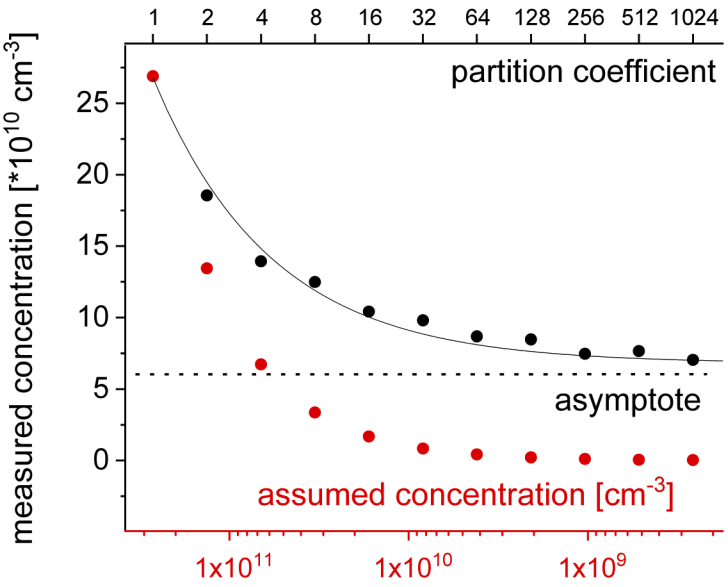

Fig. 8. Results of formaldehyde dilution in nitrogen.

Biomedical Optics EXPRESS

one. The measurement of the concentration was performed again. This operation was repeated several times.

The results of this experiment are shown in Fig. 8. It is evident that it failed to achieve a step to step partition with the coefficient of 2. Only the density of about $6{\cdot}10^{10}$ cm^{-3} was achieved due to 10 steps, starting from the initial formaldehyde concentration of about $2.7{\cdot}10^{11}$ cm^{-3}.

A deposit of formaldehyde in the apparatus is responsible for this effect. This compound adheres to the walls of the equipment in the form of a polymer (polioxymethylene) [81]. The polymer that was deposed on the walls at higher formaldehyde concentrations evaporates and provides gaseous H_2CO. The achievement of the density below the asymptotic value of $6{\cdot}10^{10}$ cm^{-3} due to successive divisions was not possible.

The contamination of formaldehyde sensors by polioxymethylene is a real problem when testing the concentrations at ppb level. Generally, cleaning of the equipment from this polymer might be performed by heating the equipment to the temperature of about 200 °C. This is rather impossible for the optical systems. Using lower temperatures which are acceptable for the multipass cells is useless. We stated that heating to about 70 °C together with pumping to about 10^{-5} atm or blowing the cell with pure nitrogen does not lead to any essential progress, even within several days. The other way is the use of the Mannich reaction [82], which requires admitting ammonia vapour under the atmospheric pressure.

We decided to benefit from the effect of polioxymethylene deposition and to use it for our detector testing at low formaldehyde concentrations. The cell was evacuated to the residual pressure of 10^{-7} atm and filled with pure nitrogen at 0.01 atm. We then observed H_2CO evaporated from the apparatus walls that slowly filled the sensor. The registration of the concentration was initially performed every minute, then less frequently. This result is presented in Fig. 9.

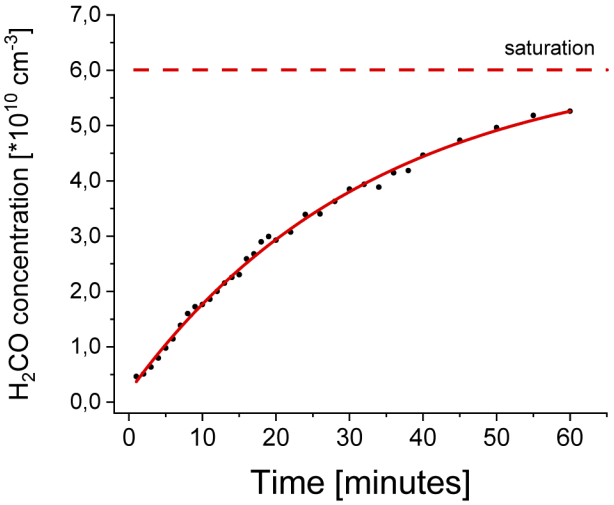

Fig. 9. Rise of formaldehyde concentration due to polioxymethylene evaporation from walls with fitted exponential growth (Eq. (2)).

Simple model of H_2CO deposition on the walls and evaporation was prepared. In this approach the density of molecules evaporating per unit of time is equal to α, while the inverse process, i.e. the number of particles adhering to apparatus surfaces is proportional to H_2CO vapour concentration (n) and deposition constant k. The evolution of the vapour concentration is then described by following differential equation:

$$\frac{dn(t)}{dt} = -kn(t) + \alpha, \tag{1}$$

Biomedical Optics EXPRESS

while its solution is in the form:

$$n(t) = \frac{\alpha}{k}[1 - \exp(-kt)]. \quad (2)$$

This function fits well to the experimental data (Fig. 9). The fitting parameters were: the deposition constant $k \approx 5{\cdot}10^{-4}\ s^{-1}$, the evaporation speed $\alpha \approx 3{\cdot}10^{7}\ \mathrm{cm^{-3}s^{-1}}$ and the saturation concentration: $\alpha/k \approx 6{\cdot}10^{10}\ \mathrm{cm^{-3}}$. Note that this value is similar to the asymptotic concentration achieved in a previous experiment where the consecutive density partition was applied.

One can evaluate using Eq. (2) that due to the polioxymethylene evaporation the sensor was filled to a H_2CO concentration of about $1{,}8{\cdot}10^{9}\ \mathrm{cm^{-3}}$ within the first minute of the measurement. This corresponds to the mixing ratio of about 6.6 ppb. This is a minimal value of formaldehyde concentration which might be generated in our experiment. Various other approaches (like attempts to clean the cell by Mannich reaction and then filing it by a correspondingly small portion of formaldehyde) were not successful since H_2CO density in the sample was temporary unstable due to adhesion of these constituents to the walls. From where else these attempts ensured us, the detection limit of our sensor was much lower than 6.6 ppb.

4. Conclusion

We present the optical sensor of formaldehyde. Its primary design is to search for the cancer biomarker in air exhaled from human lungs. Multipass absorption spectroscopy was applied. The selection of the spectral range (3595.77 - 3596.20 nm), and the use of sample pressure reduced to 0.01 atm, enabled to immunize the detection against typical interferents present in breath at high concentration including water vapour, carbon dioxide and methane, as well as other constituents. The method of optical fringes quenching and a proprietary approach to signal analysis were presented. The use of such approaches made it possible to achieve a detection limit below 1.8•109 cm-3 (6.6 ppb), which is more than sufficient to detect the morbid level of this biomarker in breath.

Funding

Narodowe Centrum Nauki (2016/23/B/ST7/03441).

Disclosures

The authors declare no conflicts of interest.

References

1. L. Zhang, G. Tian, J. Li, and B. Yu, "Applications of absorption spectroscopy using quantum cascade lasers," Appl. Spectrosc. **68**(10), 1095–1107 (2014)..
2. M. S. Zahniser, D. D. Nelson, J. B. McManus, S. C. Herndon, E. C. Wood, and J. H. Shorter, . . . & S. Park (2009, January).
3. "Infrared QC laser applications to field measurements of atmospheric trace gas sources and sinks in environmental research: enhanced capabilities using continuous wave QCLs," In *Quantum Sensing and Nanophotonic Devices VI* (Vol. 7222, p. 72220H). International Society for Optics and Photonics.
4. A. Elia, P. M. Lugarà, C. Di Franco, and V. Spagnolo, "Photoacoustic techniques for trace gas sensing based on semiconductor laser sources," Sensors **9**(12), 9616–9628 (2009)..
5. World Health Organization, *Concise International Chemical Assessment Document 40: Formaldehyde*. (World Health Organization, 2002).
6. I. M. Ritchie and R. G. Lehnen, "Formaldehyde-related health complaints of residents living in mobile and conventional homes," Am. J. Public Health **77**(3), 323–328 (1987)..
7. T. Malaka and A. M. Kodama, "Respiratory health of plywood workers occupationally exposed to formaldehyde," Arch. Environ. Health **45**(5), 288–294 (1990)..
8. T. Salthammer, S. Mentese, and R. Marutzky, "Formaldehyde in the indoor environment," Chem. Rev. **110**(4), 2536–2572 (2010)..

Biomedical Optics EXPRESS

9. P. R. Chung, C. T. Tzeng, M. T. Ke, and C. Y. Lee, "Formaldehyde gas sensors: a review," Sensors **13**(4), 4468–4484 (2013)..
10. K. T. Morgan, "A brief review of formaldehyde carcinogenesis in relation to rat nasal pathology and human health risk assessment," Toxicol. Pathol. **25**(3), 291–305 (1997)..
11. J. K. McLaughlin, "Formaldehyde and cancer: a critical review," Int. Arch. Occup. Environ. Health **66**(5), 295–301 (1994)..
12. J. A. German and M. B. Harper, "Environmental control of allergic diseases," American Family Physician **66**(3), 421 (2002).
13. E. Von Mutius, "Environmental factors influencing the development and progression of pediatric asthma," J. Allergy Clin. Immunol. **109**(6), S525–S532 (2002)..
14. V. J. Feron and H. P. Til, "Vrijer Flora de, RA Woutersen, FR Cassee, PJ van Bladeren," Mutat. Res., Genet. Toxicol. Test. **259**(3-4), 363–385 (1991)..
15. W. J. Kim, N. Terada, T. Nomura, R. Takahashi, S. D. Lee, J. H. Park, and A. Konno, "Effect of formaldehyde on the expression of adhesion molecules in nasal microvascular endothelial cells: the role of formaldehyde in the pathogenesis of sick building syndrome," Clin. Exp. Allergy **32**(2), 287–295 (2002)..
16. J. Chen, S. So, H. Lee, M. P. Fraser, R. F. Curl, T. Harman, and F. K. Tittel, "Atmospheric formaldehyde monitoring in the Greater Houston area in 2002," Appl. Spectrosc. **58**(2), 243–247 (2004)..
17. World Health Organization, *Air Quality Guidelines: Global Update 2005: Particulate Matter, Ozone, Nitrogen Dioxide, and Sulfur Dioxide* (World Health Organization, 2006).
18. B. P. Wert, M. Trainer, A. Fried, T. B. Ryerson, B. Henry, W. Potter, and G. J. Frost, "Signatures of terminal alkene oxidation in airborne formaldehyde measurements during TexAQS 2000," J. Geophys. Res.: Atmos. **108**(D3), 2502 (2003).
19. C. Wang and P. Sahay, "Breath analysis using laser spectroscopic techniques: breath biomarkers, spectral fingerprints, and detection limits," Sensors **9**(10), 8230–8262 (2009)..
20. A. Wehinger, A. Schmid, S. Mechtcheriakov, M. Ledochowski, C. Grabmer, G. A. Gastl, and A. Amann, "Lung cancer detection by proton transfer reaction mass-spectrometric analysis of human breath gas," Int. J. Mass Spectrom. **265**(1), 49–59 (2007)..
21. M. P. Fernandes, S. Venkatesh, and B. G. Sudarshan, "Early detection of lung cancer using nano-nose-a review," Open Biomed. Eng. J. **9**(1), 228–233 (2015)..
22. P. Fuchs, C. Loeseken, J. K. Schubert, and W. Miekisch, "Breath gas aldehydes as biomarkers of lung cancer," Int. J. Cancer **126**(11), 24970 (2009).
23. J. H. Miller, Y. A. Bakhirkin, T. Ajtai, F. K. Tittel, C. J. Hill, and R. Q. Yang, "Detection of formaldehyde using off-axis integrated cavity output spectroscopy with an interband cascade laser," Appl. Phys. B **85**(2-3), 391–396 (2006)..
24. C. B. Hirschmann, J. Lehtinen, J. Uotila, S. Ojala, and R. L. Keiski, "Sub-ppb detection of formaldehyde with cantilever enhanced photoacoustic spectroscopy using quantum cascade laser source," Appl. Phys. B **111**(4), 603–610 (2013)..
25. P. R. Chung, C. T. Tzeng, M. T. Ke, and C. Y. Lee, "Formaldehyde gas sensors: a review," Sensors **13**(4), 4468–4484 (2013)..
26. S. E. Ebeler, A. J. Clifford, and T. Shibamoto, "Quantitative analysis by gas chromatography of volatile carbonyl compounds in expired air from mice and human," J. Chromatogr., Biomed. Appl. **702**(1-2), 211–215 (1997)..
27. S. Costa, C. Costa, J. Madureira, V. Valdiglesias, A. Teixeira-Gomes, P. G. de Pinho, and J. P. Teixeira, "Occupational exposure to formaldehyde and early biomarkers of cancer risk, immunotoxicity and susceptibility," Environ. Res. **179**, 108740 (2019)..
28. B. Mann and M. L. Grayeski, "New chemiluminescent derivatizing agent for the analysis of aldehydes and ketones by high-performance liquid chromatography with peroxyoxalate chemiluminescence," J. Chromatogr. A **386**, 149–158 (1987)..
29. J. O. Levin, K. Andersson, R. Lindahl, and C. A. Nilsson, "Determination of sub-part-per-million levels of formaldehyde in air using active or passive sampling on 2, 4-dinitrophenylhydrazine-coated glass fiber filters and high-performance liquid chromatography," Anal. Chem. **57**(6), 1032–1035 (1985)..
30. J. Rudnicka, M. Walczak, T. Kowalkowski, T. Jezierski, and B. Buszewski, "Determination of volatile organic compounds as potential markers of lung cancer by gas chromatography–mass spectrometry versus trained dogs," Sens. Actuators, B **202**, 615–621 (2014)..
31. J. R. Hopkins, T. Still, S. Al-Haider, I. R. Fisher, A. C. Lewis, and P. W. Seakins, "A simplified apparatus for ambient formaldehyde detection via GC-pHID," Atmos. Environ. **37**(18), 2557–2565 (2003)..
32. T. Dumas, "Determination of formaldehyde in air by gas chromatography," J. Chromatogr. A **247**(2), 289–295 (1982)..
33. J. M. Lorrain, C. R. Fortune, and B. Dellinger, "Sampling and ion chromatographic determination of formaldehyde and acetaldehyde," Anal. Chem. **53**(8), 1302–1305 (1981)..
34. C. Y. Lee, C. M. Chiang, Y. H. Wang, and R. H. Ma, "A self-heating gas sensor with integrated NiO thin-film for formaldehyde detection," Sens. Actuators, B **122**(2), 503–510 (2007)..
35. J. Wang, P. Zhang, J. Q. Qi, and P. J. Yao, "Silicon-based micro-gas sensors for detecting formaldehyde," Sens. Actuators, B **136**(2), 399–404 (2009)..

Biomedical Optics EXPRESS

36. J. Wang, L. Liu, S. Y. Cong, J. Q. Qi, and B. K. Xu, "An enrichment method to detect low concentration formaldehyde," Sens. Actuators, B **134**(2), 1010–1015 (2008)..
37. M. Hämmerle, E. A. Hall, N. Cade, and D. Hodgins, "Electrochemical enzyme sensor for formaldehyde operating in the gas phase," Biosens. Bioelectron. **11**(3), 239–246 (1996)..
38. Q. Ma, H. Cui, and X. Su, "Highly sensitive gaseous formaldehyde sensor with CdTe quantum dots multilayer films," Biosens. Bioelectron. **25**(4), 839–844 (2009)..
39. G. R. Möhlmann, "Formaldehyde detection in air by laser-induced fluorescence," Appl. Spectrosc. **39**(1), 98–101 (1985)..
40. M. Cazorla, G. M. Wolfe, S. A. Bailey, A. K. Swanson, H. L. Arkinson, and T. F. Hanisco, "A new airborne laser-induced fluorescence instrument for in situ detection of formaldehyde throughout the troposphere and lower stratosphere," Atmos. Meas. Tech. **8**(2), 541–552 (2015)..
41. J. R. Hottle, A. J. Huisman, J. P. DiGangi, A. Kammrath, M. M. Galloway, K. L. Coens, and F. N. Keutsch, "A laser induced fluorescence-based instrument for in-situ measurements of atmospheric formaldehyde," Environ. Sci. Technol. **43**(3), 790–795 (2009)..
42. J. C. Septon and J. C. Ku, "Workplace air sampling and polarographic determination of formaldehyde," Am. Ind. Hyg. Assoc. J. **43**(11), 845–852 (1982)..
43. J. Wojtas, F. K. Tittel, T. Stacewicz, Z. Bielecki, R. Lewicki, J. Mikolajczyk, and J. Tarka, "Cavity-enhanced absorption spectroscopy and photoacoustic spectroscopy for human breath analysis," Int. J. Thermophys. **35**(12), 2215–2225 (2014)..
44. A. O'Keefe and D. A. Deacon, "Cavity ring-down optical spectrometer for absorption measurements using pulsed laser sources," Rev. Sci. Instrum. **59**(12), 2544–2551 (1988)..
45. K. W. Busch and M. A. Busch, eds., *Cavity-ringdown Spectroscopy: An Ultratrace-absorption Measurement Technique* (American Chemical Society, 1999).
46. J. H. Van Helden, R. Peverall, G. A. D. Ritchie, G. Berden, and R. Engeln, *Cavity Enhanced Techniques using Continuous Wave Lasers* (Wiley-Blackwell, 2009). (pp. 27–56).
47. J. Wojtas, Z. Bielecki, T. Stacewicz, J. Mikołajczyk, and M. Nowakowski, "Ultrasensitive laser spectroscopy for breath analysis," Opto-Electron. Rev. **20**(1), 26–39 (2012)..
48. T. Stacewicz, J. Wojtas, Z. Bielecki, M. Nowakowski, J. Mikołajczyk, R. Mędrzycki, and B. Rutecka, "Cavity ring down spectroscopy: detection of trace amounts of substance," Opto-Electron. Rev. **20**(1), 53–60 (2012)..
49. A. C. Tam, "Applications of photoacoustic sensing techniques," Rev. Mod. Phys. **58**(2), 381–431 (1986)..
50. C. B. Hirschmann, J. Lehtinen, J. Uotila, S. Ojala, and R. L. Keiski, "Sub-ppb detection of formaldehyde with cantilever enhanced photoacoustic spectroscopy using quantum cascade laser source," Appl. Phys. B **111**(4), 603–610 (2013)..
51. P. Patimisco, G. Scamarcio, F. K. Tittel, and V. Spagnolo, "Quartz-enhanced photoacoustic spectroscopy: a review," Sensors **14**(4), 6165–6206 (2014)..
52. J. U. White, "Long optical paths of large aperture," J. Opt. Soc. Am. **32**(5), 285–288 (1942)..
53. D. R. Herriott and H. J. Schulte, "Folded optical delay lines," Appl. Opt. **4**(8), 883–889 (1965)..
54. B. Buszewski, D. Grzywinski, T. Ligor, T. Stacewicz, Z. Bielecki, and J. Wojtas, "Detection of volatile organic compounds as biomarkers in breath analysis by different analytical techniques," Bioanalysis **5**(18), 2287–2306 (2013)..
55. L. S. Rothman, I. E. Gordon, Y. Babikov, A. Barbe, D. C. Benner, P. F. Bernath, and A. Campargue, "The HITRAN2012 molecular spectroscopic database," J. Quant. Spectrosc. Radiat. Transfer **130**, 4–50 (2013)..
56. S. Lundqvist, P. Kluczynski, R. Weih, M. von Edlinger, L. Nähle, M. Fischer, and J. Koeth, "Sensing of formaldehyde using a distributed feedback interband cascade laser emitting around 3493 nm," Appl. Opt. **51**(25), 6009–6013 (2012)..
57. Y. Mine, N. Melander, D. Richter, D. G. Lancaster, K. P. Petrov, R. F. Curl, and F. K. Tittel, "Detection of formaldehyde using mid-infrared difference-frequency generation," Appl. Phys. B: Lasers Opt. **65**(6), 771–774 (1997)..
58. S. Friedfeld, M. Fraser, D. Lancaster, D. Leleux, D. Rehle, and F. Tittel, "Field intercomparison of a novel optical sensor for formaldehyde quantification," Geophys. Res. Lett. **27**(14), 2093–2096 (2000)..
59. D. G. Lancaster, A. Fried, B. Wert, B. Henry, and F. K. Tittel, "Difference-frequency-based tunable absorption spectrometer for detection of atmospheric formaldehyde," Appl. Opt. **39**(24), 4436–4443 (2000)..
60. D. Rehle, D. Leleux, M. Erdelyi, F. Tittel, M. Fraser, and S. Friedfeld, "Ambient formaldehyde detection with a laser spectrometer based on difference-frequency generation in PPLN," Appl. Phys. B **72**(8), 947–952 (2001)..
61. A. Fried, Y. Wang, C. Cantrell, B. Wert, J. Walega, B. Ridley, and J. Hannigan, "Tunable diode laser measurements of formaldehyde during the TOPSE 2000 study: Distributions, trends, and model comparisons," J. Geophys. Res.: Atmos. **108**(D4), 8365 (2003).
62. B. P. Wert, M. Trainer, A. Fried, T. B. Ryerson, B. Henry, W. Potter, and G. J. Frost, "Signatures of terminal alkene oxidation in airborne formaldehyde measurements during TexAQS 2000," J. Geophys. Res.: Atmos. **108**(D3), 2502 (2003).
63. J. H. Miller, Y. A. Bakhirkin, T. Ajtai, F. K. Tittel, C. J. Hill, and R. Q. Yang, "Detection of formaldehyde using off-axis integrated cavity output spectroscopy with an interband cascade laser," Appl. Phys. B **85**(2-3), 391–396 (2006)..
64. G. Peach, "Theory of the pressure broadening and shift of spectral lines," Adv. Phys. **30**(3), 367–474 (1981)..

Biomedical Optics EXPRESS

65. W. Demtröder, *Laser Spectroscopy: Basic Concepts and Instrumentation* (Springer Science & Business Media, 1988).
66. J. A. Silver and A. C. Stanton, "Optical interference fringe reduction in laser absorption experiments," Appl. Opt. **27**(10), 1914–1916 (1988)..
67. J. B. McManus and P. L. Kebabian, "Narrow optical interference fringes for certain setup conditions in multipass absorption cells of the Herriott type," Appl. Opt. **29**(7), 898–900 (1990)..
68. M. Mangold, B. Tuzson, and L Emmenegger, U.S. Patent No. 9,638,624. Washington, DC: U.S. Patent and Trademark Office (2017).
69. B. Tuzson, M. Mangold, H. Looser, A. Manninen, and L. Emmenegger, "Compact multipass optical cell for laser spectroscopy," Opt. Lett. **38**(3), 257–259 (2013)..
70. H. D. Kronfeldt, "Piezo-enhanced multireflection cells applied for in-situ measurements of trace-gas concentrations," In *Lens and Optical Systems Design* (Vol. 1780, p. 17801L) (1993, April). International Society for Optics and Photonics.
71. A. Fried, J. R. Drummond, B. Henry, and J. Fox, "Reduction of interference fringes in small multipass absorption cells by pressure modulation," Appl. Opt. **29**(7), 900–902 (1990)..
72. V. V. Liger, "Optical fringes reduction in ultrasensitive diode laser absorption spectroscopy," Spectrochim. Acta, Part A **55**(10), 2021–2026 (1999)..
73. C. R. Webster, "Brewster-plate spoiler: a novel method for reducing the amplitude of interference fringes that limit tunable-laser absorption sensitivities," J. Opt. Soc. Am. B **2**(9), 1464–1470 (1985)..
74. L. Lee, H. Park, K. H. Ko, T. S. Kim, and D. Y. Jeong, "Reduction of fringe noise in a multi-pass absorption cell by using the wavelength modulation technique," J. Korean Phys. Soc. **57**(2(1)), 364–368 (2010).
75. S. Schilt, F. K. Tittel, and K. P. Petrov, "Diode laser spectroscopic monitoring of trace gases," in *Encyclopedia of Analytical Chemistry: Applications, Theory and Instrumentation* (Wiley, 2006).
76. K. Krzempek, M. Jahjah, R. Lewicki, P. Stefański, S. So, D. Thomazy, and F. K. Tittel, "CW DFB RT diode laser-based sensor for trace-gas detection of ethane using a novel compact multipass gas absorption cell," Appl. Phys. B **112**(4), 461–465 (2013)..
77. W. Ren, L. Luo, and F. K. Tittel, "Sensitive detection of formaldehyde using an interband cascade laser near 3.6 μm," Sens. Actuators, B **221**, 1062–1068 (2015)..
78. L. Dong, Y. Yu, C. Li, S. So, and F. K. Tittel, "Ppb-level formaldehyde detection using a CW room-temperature interband cascade laser and a miniature dense pattern multipass gas cell," Opt. Express **23**(15), 19821–19830 (2015)..
79. J. Li, U. Parchatka, and H. Fischer, "A formaldehyde trace gas sensor based on a thermoelectrically cooled CW-DFB quantum cascade laser," Anal. Methods **6**(15), 5483–5488 (2014)..
80. X. Zhu and D. T. Cassidy, "Electronic subtracter for trace-gas detection with InGaAsP diode lasers," Appl. Opt. **34**(36), 8303–8308 (1995)..
81. J. R. Braswell, D. R. Spiner, and R. K. Hoffman, "Adsorption of formaldehyde by various surfaces during gaseous decontamination," Appl. Microbiol. **20**(5), 765–769 (1970)..
82. M. Arend, B. Westermann, and N. Risch, "Modern variants of the Mannich reaction," Angew. Chem., Int. Ed. **37**(8), 1044–1070 (1998)..